CYP2D6 in the brain: Genotype effects on resting brain perfusion

Julia Kirchheiner, MD[1], Angela Seeringer, MD[1], Ana Leonor Godoy[1,5], Barbara Ohmle[1], Christiane Maier, PhD[2], Petra Beschoner, MD[3,4], Eun-Jin Sim, PhD[3], Roberto Viviani, PhD[3]

[1] Institute of Pharmacology of Natural Products and Clinical Pharmacology
[2] Institute of Human Genetics,
[3] Department of Psychiatry and Psychotherapy III,
[4] Department of Psychosomatic Medicine and Psychotherapy,
University of Ulm, Germany
5 Faculty of Pharmaceutical Sciences de Ribeirão Preto, University Ribeirão Preto, Brasil

Corresponding author:
Julia Kirchheiner
Institute of Pharmacology of Natural Products and Clinical Pharmacology
University of Ulm
Helmholtzstr. 20
D-89081 Ulm, Germany
Phone: +49-731-50065603
Fax: +49-731-50065605

This is the author's version of the following paper, J. Kirchheiner, A. Seeringer, A. L. Godoy, C. Maier, P. Beschoner, E. J. Sim, R. Viviani, 'CYP2D6 in the brain: Genotype effects on resting brain perfusion,' Molecular Psychiatry 16 (2011): 333-341. DOI:10.1038/mp.2010.42. Link: http://www.nature.com/mp/journal/v16/n3/full/mp201042a.html.

Abstract

The cytochrome P450 2D6 (CYP2D6) is a genetically polymorphic enzyme involved in the metabolism of several psychoactive drugs. Beside its expression in the liver, CYP2D6 is highly expressed in several regions of the brain such as the hippocampus, thalamus, hypothalamus, and the cortex, but its function in the brain is not well understood. CYP2D6 may also play a physiological role due to its involvement in neurotransmitter biotransformation. In this study, *CYP2D6* genotyping was performed in *N*=188 healthy individuals and compared to brain perfusion levels at rest, which may reflect an ongoing biological processes regulating the reactivity of the individual to emotional stimuli and the detection of signals evoking fear. Relative to *N*=42 matched extensive metabolizers, *N*=14 poor metabolizers were associated with 15% higher perfusion levels in the thalamus (p=0.03 and 0.003). Effects were also present in the whole *N*=188 sample divided into metabolizer groups, or finely graded into seven CYP2D6 activity levels. A weaker effect was observed in the right hippocampus (p=0.05). An exploratory analysis extended to the whole brain suggested involvement of CYP2D6 in regions associated with alertness or serotonergic function. These findings support the hypothesis of a functional role of CYP2D6 in the brain.

Keywords: CYP2D6, resting brain perfusion, arterial spin labelling

CYP2D6 in the brain: Genotype effects on resting brain perfusion

Introduction

CYP2D6 is an enzyme involved in the metabolism of many drugs active in the central nervous system, such as antidepressants, antipsychotics, and central opioids.[1] CYP2D6 is coded by a polymorphic gene, with 7% of the Caucasian population showing no enzymatic activity ('poor metabolizers'). 20-30% of Caucasians carry one active and one inactive allele and show intermediate enzyme activity (here referred to as 'intermediate metabolizers').[2] Individuals carrying two active alleles are 'extensive metabolizers'. Beside its expression in the liver, CYP2D6 is widely expressed in the brain, but its function there is not well understood. In man, *CYP2D6* mRNA and protein have been shown to be expressed in neurons, with preferential localization in the hippocampal cortex, thalamus, hypothalamus, substantia nigra, cerebellum, and layers III and V of neocortex.[3]

Hypotheses on the role of CYP2D6 in the brain vary.[4] CYP2D6 has been shown in *in vitro* studies to play a role in the biotransformation of precursors to endogenous transmitters such as serotonin and dopamine.[5,6] Recently, it has also been shown that CYP2D6 may play a role in morphine biosynthesis[7] and in the metabolism of the endocannabinoid anandamide.[8] However, evidence of increased regional expression in alcoholism[9] and under nicotine administration[10,11] suggests a role in the extrahepatic biotransformation of exogenous substances, analogous to its role in the liver.

Based on these findings, some studies have attempted to establish an association between a personality phenotype and *CYP2D6* genotype.[12-14] Specifically, the poor metabolizer phenotype is thought to be associated with an anxious personality trait.[15,16] However, no consistent phenotype has been detected in other studies.[17-20] Therefore, current

knowledge of the role of CYP2D6 is limited to its biochemical function, but lacks any specification of an *in vivo* phenotype. Studies of the putative effects of CYP2D6 genotype in man have attempted to identify its phenotype at a very general behavioural or personality trait level, while studies attempting to localize these possible effects in terms of characterized neurobiological systems have not been performed, thus failing to make use of neuroanatomical knowledge of its preferential expression.

When measured at rest, brain perfusion is a well-characterized index of cerebral activity[21-23] thought to support the capacity of the individual to react to environmental stimuli quickly and specifically.[24] This functional interpretation of rest perfusion depends on the observation of its modulation in specific structures in the wake-sleep cycle[25,26] as well as during pathological states such as depression[27,28] which may also be viewed as conditions of altered vigilance for specific classes of environmental stimuli.[29] Furthermore, considerable variation in rest perfusion levels is present in normal individuals[30] some of which may be associated with personality traits,[31] or with genetic polymorphisms with possible relevance for vulnerability to depression and anxiety.[32,33] However, a significant portion of the variance in perfusion levels between individuals has yet to be explained.

In this study we used an advanced arterial spin labelling technique (continuous arterial spin labelling, CASL[34]) to seek the influence of *CYP2D6* polymorphism in the levels of resting brain perfusion. To increase the power of the study, we focused on two *a priori* defined regions of interest, the hippocampus and the thalamus, where this gene is preferentially expressed and the CASL signal is reliable. We also included the basal ganglia as a control region where the perfusion rate should have been unaffected by *CYP2D6* genotype.[3,9] This first analysis was followed by an explorative analysis of the effects of *CYP2D6* polymorphism in the whole brain.

Materials and Methods

Sample selection

Participants of central European origin were recruited from local schools and university and by local announcements. Exclusion criteria were neurological or medical conditions, use of medication, alcohol or drug abuse or a history of mental illness, and the presence of subclinical structural abnormalities in standard clinical imaging. The sample thus obtained was described in ref. 30, and consists of resting perfusion data collected with the same methodology in three studies after obtaining informed consent to both image acquisition and genotyping. Blind to genotype, perfusion images were individually checked for the presence of movement artefacts or problems in the quantification of CBF, discarding 3 participants. Other participants gave no consent to genotyping, leaving a sample of $N = 188$ in which *CYP2D6* genotype could be determined. The study protocol was approved by the institutional ethical committee and was performed in compliance with national legislation and the Code of Ethical Principles for Medical Research Involving Human Subjects of the World Medical Association.

Genotyping

CYP2D6 genotyping was performed for detecting the inactive alleles CYP2D6*3, *4, *5, *6, and the gene duplication as well as the decreased activity alleles CYP2D6*9, *10, *17 and *41 and the high activity alleles *2, *35. Genotyping was performed with a combination of long PCR and primer-extension method using the SNaPshot-Kit®, Applied Biosystems, Mannheim, Germany as described elsewhere.[35,36] The sequence between exon 9 of the upstream and intron 2 of the downstream *CYP2D6* gene copy of the duplicated *CYP2D6* allele was amplified using duplication specific long PCR. The PCR reaction was performed using primer set CYP2D6-F: 5′-CCA GAA GGC TTT GCA GGC TTC A- 3′ and CYP2D6-R: 5′-ACT GAG CCC TGG GAG GTA GGT A-3′ and Expand Long Template PCR System (Roche, Mannheim, Germany) as follows: in a total volume of 25µl, 2.8µl of buffer 1 of the

long PCR kit was added, supplemented with 0.4µl of 50mM $MgCl_2$, 4.5µl of 2mM dNTPs, 0.5µl of each 10µM primer and 0.3µl polymerase mix were incubated for 2 min at 94 °C, followed by 35 cycles (10 sec at 96 °C, 20 sec at 60 °C and 5 min at 68 °C) and 7 min at 68 °C. The PCR product was used as a template for the SNaPshot reaction, which was designed to genotype the polymorphic positions 2850C>T, 1846G>A, 1707 T deletion, 2613 deletion of AGA, 100C>T, 4180G>C, 1023C>T, 2988G>A, 31 G>A, and 2549 A deletion (Primers: 2850 C>T, 5'−(A)7CAGGTCAGCCACCACTATGC−3'; 1846 G>A, 5'−(A)16TACCCGCATCTCCCACCCCCA−3'; 1707 deletion T, 5'−(A)21GGCAAGAAGTCGCTGGAGCAG−3'; 2613 deletion of AGA, 5'−(A)26GCCTTCCTGGCAGAGATGGAG−3'; 100C>T, 5'−(A)31CAACGCTGGGCTGCACGCTAC−3'; 4180G>C, 5'−(A)37CAAAGCTCATAGGGGGATGGG−3'; 1023C>T, 5'−(A)42CCGCCCGCCTGTGCCCATCA−3'; 2988G>A, 5'−(A)47CAGTGCAGGGGCCGAGGGAG−3'; 31 G>A, 5'−(A)43CCAGGAGCAGGAAGATGGCCACTATCA−3', and 2549 A deletion, 5'−(A)54GGGCTGGGTCCCAGGTCATCC−3'). The SNaPshot reactions were performed according to the manufacturer's instructions (Applied Biosystems, Weiterstadt, Germany).

To code the phenotype, genotypes were assigned to three groups according to the number of deficient activity alleles (CYP2D6*3, *4, *5, *6), resulting into a *CYP2D6* poor metabolizer phenotype for carriers of two deficient activity alleles, an intermediate metabolizer phenotype for individuals with one deficient activity allele, and an extensive metabolizer phenotype for individuals lacking any deficient activity allele. The CYP2D6 activity score was calculated according to the methods published earlier.[37]

Image acquisition and preprocessing

All magnetic resonance imaging (MRI) data were obtained with a 3-Tesla Magnetom Allegra (Siemens, Erlangen, Germany) MRI system equipped with a head volume coil. All participants were scanned at the Department of Psychiatry of the University of Ulm. A standard T2-weighted structural brain scan from the clinical screening routine in use in our hospital (TR 4120, TE 82) was taken on all participants to exclude subclinical structural

abnormalities. During the measurement of baseline perfusion, participants were asked to lie quietly in the scanner with closed eyes without falling asleep. A continuous arterial spin-labeling technique was used as described in ref. 34. Interleaved images with and without labeling were acquired for 8 min (120 scans) by using a gradient-echo echo-planar imaging sequence with a field of view of 22 cm. Image size was 64 × 64 × 15 voxels, slice thickness 6 mm with a gap of 1.5 mm, giving a voxel size of 3.44 × 3.44 × 7.50 mm. The images were acquired with an echo-planar imaging sequence (EPI) with TR 4000, TE 17, anterior-to-posterior phase encoding, a flip angle of 90°, and a bandwidth of 3005 Hz/Pixel. A delay of 1 sec was inserted between the end of the labeling pulse and image acquisition to reduce transit artefacts.

The SPM2 package was used (Wellcome Department of Cognitive Neurology, London; online at http://www.fil.ion.ucl.ac.uk) for realignment and stereotactic normalization to an EPI template (Montreal Neurological Institute, resampling size: 2 × 2 × 2 mm). Reconstruction of rCBF values was obtained using software implementing equation (1) of ref. 38. The 'simple subtraction' method was used. All volumes were smoothed using an isotropic Gaussian kernel of full width half-maximum (FWHM) 8 mm. For the whole brain analysis, an explicit mask was obtained by thresholding the *a priori* thresholded tissue probability maps provided by the SPM package at 0.25 for gray or white matter. The cerebellar region and the lower brainstem were excluded manually in this mask because affected by large variance, which may be of artefactual nature in our images (these regions are close to where the labelling pulse is given). For the *a priori* region of interest analyses, anatomical regions (hippocampus and thalamus, basal ganglia including putamen, globus pallidus, and nucleus caudatus) were drawn using the map 'aal.img' shipped with the freely available programme MRIcroN, obtained from the website www.sph.sc.edu/comd/rorden/mricron/.

Statistical analysis

Effect of *CYP2D6* genotype was first tested in two regions of interest selected a priori based on published expression studies,[3,9] and then on the whole brain in a second analysis with exploratory character, using the statistical mapping approach[39]. Because the frequency of poor metabolizers, where the effect may be strongest, is very low in the population, and the multiple effect on CYP2D6 activity by multiallelic variation may not be linear, we employed matching[40,41] to select a sample contrasting poor with extensive metabolizers. We then used the full sample to characterize the shape of the effect of the whole genotypic variational spectrum in the region of interest where the effect detected by the matched analysis was strongest.

The matched sample was obtained by matching the 14 individuals with two alleles coding deficient enzyme activity (poor metabolizers) with 42 individuals without any deficient activity allele (extensive metabolizers) by age, sex, the time in which scan was conducted (rated in months) and study (since images were acquired in two main batches) using the freely available program MatchIt, obtained from the website www.stat.lsa.umich.edu/~bbh/optmatch.html.[42,43] Matching 1 poor metabolizer to 3 extensive metabolizers was done in order to improve the detection power and reduce model dependence (ref. 41, Chapter 10; 44). After matching, participants with these two genotypes did not significantly differ in sex (logistic regression, $z = 0.45$, $p = 0.7$, two-tailed), age ($z = 0.19$, $p = 0.8$), scan period ($z = -0.23$, $p = 0.8$) or study ($z = -0.01$, $p = 0.99$). The 'optimal matching' algorithm was used.[41,44] This and other univariate models were estimated with the freely available statistical programme R (version 2.9.2, available from www.r-project.org, The R Foundation for Statistical Computing, Vienna).

The model used to analyze CBF data included *CYP2D6* phenotype as the primary covariate of interest, and age, sex, scan period, and study as nuisance covariates. After checking that it was not associated with *CYP2D6* phenotype (matched sample, logistic

regression, $z = 0.45$, $p = 0.65$; whole sample, $t_{182} = 0.22$, $p = 0.82$), global CBF (the average perfusion across the brain in each individual) was also added as a nuisance covariate to the model.[45,46] The same model was used to analyze both the matched and the whole samples.

In voxel by voxel analyses using the parametric mapping approach, images of the baseline perfusion signal in each individual were averaged after preprocessing and entered at the 'second level' of analysis to model subjects as a random factor. Second level statistical analysis was performed on these averaged volumes using the same model and using a permutation method to obtain voxel-level corrected significance values.[47] Permutation tests do not rely on distributional assumptions and show generally superior power in neuroimaging applications.[48] Significance values for voxel, cluster, and set level inferences were computed based on the quantiles of the permutation distribution of the maximal *t*, the largest cluster of contiguous overthreshold voxels, and the number of overthreshold voxels, respectively. Clusters and sets were defined *a priori* by the univariate significance level 0.005, as in refs. 33 and 49, for the whole volume test, and 0.05 for tests in the regions of interest. In each test, 8000 permutations were computed. Computations were carried out in MATLAB R2006b (The Mathworks, Natick, MA) installed on a machine equipped with a 64-bit Athlon processor (Advanced Micro Devices, Sunnyvale, CA) running Windows XP (Microsoft, Redmond, WA). For the generation of random numbers, the 'MATLAB5 generator' was used. Images were generated with the same application MRIcroN used to select the anatomical regions of interest (www.sph.sc.edu/comd/rorden/mricron/).

Results

In the whole sample, 14 individuals were poor metabolizers with two alleles coding deficient enzyme activity (CYP2D6*3, *4, *5 or *6), 69 individuals were carriers of one deficient activity allele (intermediate metabolizers); the remaining 105 individuals carried no deficient activity allele (extensive metabolizers). The sample obtained through matching and the whole sample are described in Table 1.

TABLE 1 HERE

Analysis regions of interest hippocampus and thalamus

In the mean CBF analysis, perfusion levels were first averaged over the two regions of interest, hippocampus and thalamus, on the left and right side, and the basal ganglia as a control region. Tests of *CYP2D6* genotype effects in the linear model for the matched sample (poor vs. extensive metabolizers) revealed significant perfusion increases in poor metabolizers in all these regions except the left hippocampus (Table 2, left). The evidence and the size of *CYP2D6* genotype effects in the hippocampus, however, were considerably lower than in the thalamus. In this latter region, poor metabolizers were characterized by average increases of perfusion levels of 7.7 ml/100gr/min relative to extensive metabolizers (s.d. 2.7 ml/100gr/ml), corresponding to percent changes of 15% of baseline levels. No significant *CYP2D6* genotype effects were detected in the control region of the basal ganglia.

TABLE 2 HERE

Data for the whole sample are in Table 2, right. Here, the mean perfusion is slightly lower than in the matched sample due to a preponderance of female participants.[30] Its analysis confirmed the existence of a significant linear effect of increased perfusion from extensive to poor metabolizers, with average effect sizes of about 1.9 ml/100gr/ml (s.d. 1.1 ml/100gr/ml) in the hippocampus, and about 5.4 ml/100gr/ml (s.d. 2.0 ml/100gr/ml) in the thalamus (Table 2, right). This effect may also be seen in the box plots of Figure 1, which are based on the whole sample. Except for the data from the left hippocampus, perfusion levels of intermediate metabolizers lay between those of poor and extensive metabolizers. Also in the whole sample, no significant effect of CYP2D6 genotype was detected in the control region of the basal ganglia.

FIGURE 1 HERE

In Figure 2, mean CBF perfusion in the thalamus and hippocampus were plotted on the whole spectrum of allelic variation on the CYP2D6 activity score. This score attempts to

capture finely graded variation in enzymatic activity based on the combinations of the ten most common alleles with known functional relevance (see Methods), resulting in seven levels of activity.[37] In the thalamus, where the *CYP2D6* genotype effect was largest, one can see that CBF decreases with increasing CYP2D6 activity score ($t_{181} = 2.37$, $p = 0.02$, two-tailed), levelling off at midrange in a slight nonlinearity of effect. In the rest of the analysis, we continued to use a three-groups coding based on the number of deficient activity alleles (poor, intermediate, and extensive metabolizers) to test genotype effects. In the hippocampus, evidence for activity scores effects was limited ($t_{181} = 1.00$, n.s.).

FIGURE 2 HERE

The voxel by voxel analysis of the regions of interest confirmed these findings, detecting significant activations at voxel level in the comparison between poor and extensive metabolizers in the left and right thalamus, while a trend was observed in the right hippocampus (Figure 3 and 4, Table 3). Post-hoc inspection of the overlaid *t* values in the hippocampus revealed an unequal involvement of the hippocampal structure, selectively affecting the posterior and medial parts (Figure 4). In the surround, there was a tendency of the association to extend inferiorly towards the parahippocampal cortex (Figure 3, center).

FIGURE 3 AND 4 HERE

Voxel by voxel analysis extended to whole brain

In this analysis, CBF levels were regressed on *CYP2D6* genotype in the whole brain voxel by voxel to verify the possible existence of associations outside the predefined regions of interest. Set level tests yielded a significant trend for a positive association with the poor metabolizer status in the matched sample (set level: $p = 0.01$, one-tailed), which was also present in the whole sample ($p < 0.01$). The effects in individual areas reported below survived a significance threshold of $p < 0.001$, uncorrected. As one can see from the top half of Figure 3, apart from the areas of the region of interest analysis, the largest positive associations in the neocortex were found in a diffuse area extending over the calcarine and

occipital cortex (lingula, BA 18-27, $t = 4.33$ in the matched sample, $t = 4.22$ in the whole sample), in the precuneus (BA 17, $t = 3.46$ in the matched sample, $t = 3.61$ in the whole sample), and in the substantia innominata/orbitofrontal cortex (x, y, z = 18, 20, −14, $t = 4.74$, matched sample, and $t = 3.48$, whole sample). Positive associations were also noted in the hypothalamus (x, y, z = 2, −2, −10, $t = 4.12$, matched sample, and $t = 4.42$, whole sample), a structure expressing CYP2D6 at very high levels,[3] and in the raphe nucleus (x, y, z = 2, −30, −16, $t = 2.70$, matched sample, and $t = 3.99$). Effect plots for the CYP2D6 activity scores in the two areas of largest effect, the hypothalamus and the occipital/calcarine cortex, are in the bottom half of Figure 3, showing similar CBF decreases with increasing CYP2D6 activity and the tendency to level-off at midrange.

In the striatum and caudate nucleus, there was no positive association between the presence of deficient activity alleles and perfusion levels that survived the uncorrected threshold for cluster and set definition; on the contrary, perfusion levels were generally lower (x, y, z = −14, 8, −2, left pallidum, $t = -2.82$, matched sample, and $t = -2.83$, whole sample). Similarly, in the rest of the neocortex, there was a weak, diffuse negative association with poor metabolizer status ($p = 0.03$, set-level correction).

Discussion

Because of its involvement in the biotransformation of various bioactive substrates in the brain such as neurotransmitters, endogenous morphines and endocannabinoids, a functional role of CYP2D6 in the brain has been the object of much speculation. In man, however, no functional phenotype of *CYP2D6* genetic polymorphism referring to brain function has been found in support of this hypothesis. In this study, we sought an association between resting brain perfusion and metabolizer status underlying possible commonalities between the effect of *CYP2D6* polymorphism and brain perfusion at rest. The effect of *CYP2D6* genotype was estimated on resting brain perfusion in regions of interest determined by high expression levels of CYP2D6 protein and mRNA. An effect was detected in these regions as an increase

of perfusion levels in poor metabolizers. In the thalamus, where the detected effect of decreased CYP2D6 activity was largest, poor metabolizers were characterized by an increase of about 15% in perfusion levels compared to extensive metabolizers. Intermediate metabolizers lay in between. In the hippocampus, the effect was weaker and mainly affected the posterior portion, consistent with the position of the dentate gyrus, in which CYP2D6 expression is largest.[3]

Because the concentration of CYP2D6 in the brain is low and restricted to neuronal cells,[3] it is not surprising that any effect, if it exists, may be detected in areas of high neuronal density and comparably high expression levels. In this study, no effect could be detected in regions with known low or absent expression of CYP2D6 such as the caudatus or the putamen. Outside the defined regions of interest, there was some evidence for a similar genotype effect in the hypothalamus, raphe nucleus, and occipital cortex (Figure 3).

As CYP2D6 is involved in the transformation of several bioactive compounds in the brain, it is difficult to attribute any effect of *CYP2D6* genotype to a single functional pathway. One possible key for understanding the functional role of CYP2D6 comes from a recent study showing its involvement in the synthesis of endogenous morphine.[7] Poor metabolizers might have lower endorphin levels, and show higher resting brain perfusion in those regions where CYP2D6-mediated biotransformation is quantitatively important. Interestingly, the thalamus is a diencephalic nucleus also involved in nociception.[50,51] In this region, individual differences in sensitivity to pain are associated with differences in activity.[52] In addition, the thalamus is an important relay centre for the reticular ascending system, which regulates arousal and alertness.[53-55] Thalamic perfusion is associated with alertness levels[25,56] and is substantially reduced during sleep.[26] The association with perfusion levels in the substantia innominata/orbitofrontal cortex and the occipital calcarine cortex is also consistent with involvement of a network subserving alertness.[56] Therefore, our findings raise the question of

whether genotype differences may be associated with modulations of the thalamus affecting the reactivity to potentially harmful stimuli, or sustained attention/alertness.

In some studies investigating the relationship between *CYP2D6* genotype and personality, an association was found between the poor metabolizer genotype and trait anxiety.[15,16] The hippocampus has been shown to be involved in the regulation of anxiety.[57] However, only limited evidence was found for an effect of CYP2D6 activity on perfusion in this region. A possible perspective for future studies concerns the clarification of the relations between anxiety, CYP2D6, and the hippocampus.

In the exploratory analysis, CYP2D6 effects in the hypothalamus colocalized with high CYP2D6 expression levels. Because a similar effect was also observed in the raphe nucleus, and both regions are characterized by high serotonin turnover and transporter density,[58] it is possible to speculate that involvement of CYP2D6 in the serotonergic metabolism might be the mechanism at the basis of the changes in these regions.

There are several limitations potentially affecting this study. Firstly, although our sample of 188 normal participants is comparatively large for MRI standards, the occurrence rate of 7% poor metabolizers in the population[59] led to only 14 individuals being carriers of two deficient activity alleles. Secondly, as in any other observational study, unidentified covariates may be a source of hidden bias potentially affecting effect estimates.[41] Although the data were matched and adjusted for age, sex, and time of the study, we may have failed to condition for unknown variables that could conceivably have an association with individual levels of rest perfusion, such as smoking status and, less likely in our sample, heavy alcohol abuse. Smoking and alcoholism has been reported to affect CYP2D6 expression in certain regions in the brain.[9,10] However, the brain regions where CYP2D6 induction was observed in these studies (globus pallidus, substantia nigra, cerebellum) were different from those detected here.

Taken together, these findings support the hypothesis of a functional role of CYP2D6 in the brain. An interesting issue for future neuroimaging studies is the existence of effects of *CYP2D6* genotype in tasks that specifically rely on the regions found to be associated with its expression and activity. Studies identifying intermediate phenotypes will be crucial in understanding the function of CYP2D6 in the brain.

Disclosure/Conflicts of interest

Drs Kirchheiner and Seeringer report having received lecture fees from GSK, Servier and Eisai. Drs Viviani, Godoy, Ohmle, Beschoner, and Sim declare no conflict of interest.

Acknowledgments

The authors are grateful to Dr J.J. Wang from the Department of Radiology and Center for Functional Neuroimaging at University of Pennsylvania for granting us use of the CASL sequence and for providing the software for the estimation of the perfusion values. Many thanks to Dr. Georg Grön of the Department of Psychiatry of the University of Ulm for help in obtaining and setting up the CASL sequence.

References

1. Distlerath LM, Guengrich FP. Characterization of a human liver cytochrome P-450 involved in the oxidation of debrisoquine and other drugs by using antibodies raised to the analogous rat enzyme. *Proc Natl Acad Sci USA* 1984; **81**: 7348-7352.
2. Sachse C, Brockmöller J, Bauer S, Root I. Cytochrome P450 2D6 variants in a caucasian population: Allele frequencies and phenotypic consequences. *Am J Med Hum Genet* 1997; **60**: 284-295.
3. Siegle I, Fritz P, Eckhardt K, Zanger UM, Eichelbaum M. Cellular localization and regional distribution of CYP2D6 mRNA and protein expression in human brain. *Pharmacogenetics* 2001; **11**: 237-245.

4. Dorado P, Peñas-Lledó EM, Llerena A. CYP2D6 polymorphism: Implications for antipsychotic drug response, schizophrenia and personality traits. *Pharmacogenomics* 2007; **8**: 1597-1608.

5. Hiroi T, Imaoka S, Funae Y. Dopamine formation from tyramine by CYP2D6. *Biochem Biophys Res Commun* 1998; **249**: 838-843.

6. Yu AM, Idle JR, Byrd LG, Krausz KW, Küpfer A, Gonzalez FJ. Regeneration of serotonin from 5-methoxytryptamine by polymorphic human CYP2D6. *Pharmacogenetics* 2003; **13**: 173-181.

7. Zhu W. CYP2D6: A key enzyme in morphine synthesis in animals. *Med Sci Monit* 2008; **14**: SC15-SC18.

8. Snider NT, Sikora MJ, Sridar C, Feuerstein TJ, Rae JM, Hollenberg PF. The endocannabidoid anandamide is a substrate for the human polymorphic cytochrome P450 2D6. *J Pharmacol Exp Ther* 2008; **327**: 538-545.

9. Miksys S, Rao Y, Hoffmann E, Mash DC, Tyndale RF. Regional and cellular expression of CYP2D6 in human brain: Higher levels in alcoholics. *J Neurochem* 2002; **82**: 1376-1378.

10. Mann A, Miksys S, Lee A, Mash DC, Tyndale RF. Induction of the drug metabolizing enzyme CYP2D6 in monkey brain by chronic nicotine treatment. *Neuropharmacology* 2008; **55**: 1147-1155.

11. Yue J, Miksys S, Hoffmann E, Tyndale RF. Chronic nicotine treatment induces rat CYP2D6 in the brain but not in the liver: An investigation of induction and time course. *J Psychiatry Neurosci* 2008; **33**: 54-63.

12. Gan SH, Ismail R, Wan Adnan WA, Zulmi W, Kumaraswamy N, Larmie ET. Relationship between Type A and B personality and debrisoquine hydroxylation capacity. *Br J Clin Pharmacol* 2004; **57**: 785-789.

13. Roberts RL, Luty SE, Mulder RT, Joyce PR, Kennedy MA. Association between cytochrome P450 2D6 genotype and harm avoidance. *Am J Med Genet (Neuropsychiat Genet.)* 2004; **127B**: 90-93.

14. Yasui-Furukori N, Kaneda A, Iwashima K, Saito M, Nakagami T, Tsuchimine S *et al*. Association between cytochrome P450 (CYP) 2C19 polymorphism and harm avoidance in Japanese. *Am J Med Genet (Neuropsychiat Genet.)* 2007; **144B**: 724-727.

15. González I, Peñas-Lledó EM, Pérez B, Dorado P, Alvarey M, Llerena A. Relation between CYP2D6 phenotype and genotype and personality in healthy volunteers. *Pharmacogenomics* 2008; **9**: 833-840.

16. Llerena A, Edman G, Cobaleda J, Benítez J, Schallung D, Bertilsson L. Relationship between personality and debrisoquine hydroxylation capacity. Suggestion of an endogenous neuroactive substrate or product of the cytochrome P4502D6. *Acta Psychiatr Scand* 1993; **87**: 23-28.

17. Bijl MJ, Luijendijk HJ, van den Berg J, Visser LE, van Schaik RHN, Hofman A *et al*. Association between the *CYP2D6*4* polymorphism and depression or anxiety in the elderly. *Pharmacogenomics* 2009; **10**: 541-547.

18. Kirchheiner J, Lang U, Stamm T, Sander T, Gallinat J. Association of CYP2D6 genotypes and personality traits in healthy individuals. *J Clin Psychopharmacol* 2006; **26**: 440-442.

19. Iwashima K, Yasui-Furukori N, Kaneda A, Saito M, Nakagami T, Sato Y *et al*. No association between CYP2D6 polymorphisms and personality trait in Japanese. *Br J Clin Pharmacol* 2007; **64**: 96-99.

20. Suzuki E, Kitao Y, Ono Y, Iijima Y, Inada T. Cytochrome P450 2D6 polymorphism and character traits. *Psychiatr Genet* 2003; **13**: 111-113.

21. Andreasen NC, O'Leary DS, Cizadlo T, Arnd S, Rezai K, Watkins GL *et al*. Remembering the past: Two facets of episodic memory explored with positron emission tomography. *Am J Psychiatry* 1995; **152**: 1576-1585.

22. Raichle ME, MacLeod AM, Snyder AZ, Powers WJ, Gusnard DA, Shulman GL. A default mode of brain function. *Proc Natl Acad Sci USA* 2001; **98**: 676-682.

23. Shulman GL, Fiez JA, Corbetta M, Buckner RL, Miezin FM, Raichle ME *et al*. Common blood flow changes across visual tasks II. Decreases in cerebral cortex. *J Cognitive Neurosci* 1997; **9**: 648-663.

24. Raichle ME, Gusnard DA. Intrinsic brain activity sets the stage for expression of motivated behavior. *J Comp Neurol* 2005; **493**: 167-176.

25. Coull JT. Neural correlates of attention and arousal: Insights from electrophysiology, functional neuroimaging and psychopharmacology. *Progr Neurobiol* 1998; **55**: 343-361.

26. Maquet P. Functional neuroimaging of normal human sleep by positron emission tomography. *J Sleep Res* 2000; **9**: 207-231.

27. Drevets WC. Neuroimaging studies of mood disorder. *Biol Psychiatry* 2000; **48**: 813-829.

28. Mayberg HS. Positron emission tomography imaging in depression: A neural systems perspective. *Neuroimaging Clin N Am* 2003; **13**: 805-815.

29. Davis M, Whalen PJ. The amygdala: Vigilance and emotion. *Mol Psychiatry* 2001; **6**: 13-34.

30. Viviani R, Sim EJ, Lo H, Richter S, Haffer S, Osterfeld N *et al*. Components of variance in brain perfusion and the design of studies of individual differences: The baseline study. *NeuroImage* 2009; **46**: 12-22.

31. Abler B, Hofer C, Viviani R. Habitual emotion regulation strategies and baseline brain perfusion. *NeuroReport* 2008; **19**: 21-24.

32. Canli T, Qiu M, Omura K, Congdon E, Haas BW, Amin Z *et al*. Neural correlates of epigenesis. *Proc Natl Acad Sci USA* 2006; **103**: 16033-16038.

33. Rao H, Gillihan SJ, Wang J, Korczykowski M, Sankoorikal GMV, Kaercher KA *et al*. Genetic variation in serotonin transporter alters resting brain function in healthy individuals. *Biol Psychiatry* 2007; **62**: 600-606.

34. Wang J, Zhang Y, Wolf RL, Roc AC, Alsop DC, Detre JA. Amplitude-modulated continuous arterial spin-labeling 3.0-T perfusion MR imaging with a single coil: Feasibility study. *Radiology* 2005; **235**: 218-228.

35. Heller T, Kirchheiner J, Armstrong VW, Luthe H, Tzvetkon M, Brockmöller J *et al*. AmpliChip CYP450 GeneChip®: A new gene chip that allows rapid and accurate *CYP2D6* genotyping. *Ther Drug Monit* 2006; **28**: 673-677.

36. Fuselli S, Dupanlop I, Frigato E, Cruciani F, Scozzari R, Moral P *et al*. Molecular diversity at the CYP2D6 locus in the Mediterranean region. *Eur J Hum Genet* 2004; **12**: 916-924.

37. Gaedigk A, Simon SD, Pearce RE, Bradford LD, Kennedy MJ, Leeder JS. The CYP2D6 activity score: Translating genotype information into a qualitative measure of phenotype. *Clin Pharmacol Ther* 2008; **83**: 234-242.

38. Wang J, Alsop DC, Li L, Listerud J, Gonzalez-At JB, Detre JA. Arterial transit time imaging with flow encoding arterial spin tagging (FEAST). *Magn Reson Med* 2003; **50**: 599-607.

39. Friston KJ, Holmes AP, Worsley KJ, Poline JP, Frith CD, Frackowiak RSJ. Statistical parametric maps in functional imaging: A general linear approach. *Hum Br Mapping* 1995; **2**: 189-210.

40. Rubin DB. Matching to remove bias in observational studies. *Biometrics* 1973; **29**: 159-184.

41. Rosenbaum PR. *Observational Studies*. Berlin: Springer, 2002.

42. Ho D, Imai K, King G, Stuart E. Matching as nonparametric preprocessing for reducing model dependence in parametric causal inference. *Polit Anal* 2007; **15**: 199-236.

43. Imai K, King G, Stuart EA. Misunderstandings between experimentalists and observationalists about causal inference. *J R Statist Soc A* 2008; **171**: 481-502.

44. Hansen BB. Full matching in an observational study of coaching for the SAT. *J Amer Statist Assoc* 2004; **99**: 609-618.

45. Aguirre GK, Zarahn E, D'Esposito M. The inferential impact of global signal covariates in functional neuroimaging analysis. *NeuroImage* 1998; **8**: 302-306.

46. Friston KJ, Frith CD, Liddle PF, Dolan RJ, Lammertsma AA, Frackowiak RSJ. The relationship between global and local changes in PET scans. *J Cerebr Bl Flow Metab* 1990; **10**: 458-466.

47. Holmes AP, Blair RC, Watson JDG, Ford I. Nonparametric analysis of statistic images from functional mapping experiments. *J Cerebr Bl Flow Metab* 1996; **16**: 7-22.

48. Nichols TE, Hayasaka S. Controlling the familywise error rate in functional neuroimaging: A comparative review. *Statist Meth Med Res* 2003; **12**: 419-446.

49. Viviani R, Sim EJ, Lo H, Beschoner P, Osterfeld N, Maier C *et al*. Baseline brain perfusion and the serotonin transporter promoter polymorphism. *Biol Psychiatry* 2009; **doi**: 10.1016/j.biopsych.2009.08.034 (epub ahead of print).

50. Jones AKP, Brown WD, Friston KJ, Qi LY, Frackowiak RSJ. Cortical and subcortical localization of response to pain in man using positron emission tomography. *Proc R Soc Lond B* 1991; **244**: 39-44.

51. Vogt BA, Gabriel M. *The Neurobiology of Cingulate Cortex and Limbic Thalamus*. Boston: Birkhauser, 1993.

52. Ochsner KN, Ludlow DH, Knierim K, Hanelin J, Ramachandran T, Gloval GC *et al*. Neural correlates of individual differences in pain-related fear and anxiety. *Pain* 2006; **120**: 69-77.

53. Kinomura S, Larsson J, Gulyas B, Roland PE. Activation by attention of the human reticular formation and thalamic reticular nuclei. *Science* 1996; **271**: 512-515.

54. McCormick DA. Neurotransmitter actions in the thalamus and cerebral cortex and their role in neuromodulation of thalamocortical activity. *Progr Neurobiol* 1992; **39**: 337-338.

55. Posner MI. Attention in cognitive neuroscience: An overview. In Gazzaniga MS (ed) *The Cognitive Neurosciences*. Cambridge (Mass.): MIT Press, 1995, pp. 615-624.

56. Paus T, Zatorre R, Hofle N, Caramanos Z, Gotman J, Petrides M *et al*. Time-related changes in neural systems underlying attention and arousal during the performance of an auditory vigilance task. *J Cognitive Neurosci* 1997; **9**: 392-408.

57. Gray JA, McNaughton N. *The Neuropsychology of Anxiety: An Enquiry into the Functions of the Septohippocampal System*. (2nd ed.) Oxford: Oxford University Press, 2000.

59. Bradford LD. CYP2D6 allele frequency in European Caucasians, Asians, Africans and their descendants. *Pharmacogenomics* 2002; **3**: 229-243.

60. Arvidsson U, Riedl M, Chakrabarti S, Lee JH, Nakano AH, Dado RJ *et al*. Distribution and targeting of a mu-opioid receptor (MOR1) in brain and spinal cord. *J Neurosci* 1995; **15**: 3328-3341.

58. Ichise M, Liow JS, Lu JQ, Takano A, Model K, Toyama H *et al*. Linearized reference tissue parametric imaging methods: Application to [^{11}C]-DASB positron emission tomography studies of the serotonin transporter in human brain. *J Cerebr Bl Flow Metab* 2003; **23**: 1096-1112.

Tables

Table 1. Summary statistics of samples.

	Number	Female	Age
Matched sample (poor vs. extensive metabolizers)			
Poor metabolizer	14	6 (42.9%)	24.71±1.59
Extensive metabolizer	42	15 (35.7%)	24.54±2.51
Whole sample			
Poor metabolizer	14	6 (42.9%)	24.71±4.30
Intermediate metabolizer	69	32 (46.4%)	25.42±4.23
Extensive metabolizer	105	59 (56.2%)	24.95±4.99

Table 2. Association between CYP2D6 genotype and perfusion levels in the regions of interest

	matched sample: PM vs. EM				whole sample			
Location	mean CBF	effect	*t*(49)	*p*	mean CBF	effect	*t*(181)	*p*
Regions of interest for expected effect								
Hippocampus L	51.6±10.8	0.43±1.80	0.24	n.s.	49.8±10.8	2.00±1.19	1.67	0.09
Hippocampus R	51.8±11.2	3.78±1.90	2.00	0.05	50.0±10.9	1.69±1.37	1.23	n.s.
Thalamus L	47.4±12.7	5.84±2.65	2.20	0.03	45.0±12.7	5.20±2.05	2.54	0.01
Thalamus R	46.7±13.9	9.58±3.00	3.19	0.003	45.8±12.6	5.61±2.11	2.66	0.009
Regions of interest for control								
Basal ganglia L	44.5±9.8	−1.13±1.36	−0.83	n.s.	43.0±10.3	−1.05±0.94	−1.13	n.s.
Basal ganglia R	45.5±10.4	−0.06±1.03	−0.07	n.s.	44.4±10.7	−1.10±0.88	−1.25	n.s.

Abbreviations: EM, PM: extensive, poor metabolizer; mean CBF: mean cerebral blood flow, in ml/100gr/min; effect: effects and relative standard deviations referring to the estimated increase in average perfusion levels, in ml/100gr/min, between poor and extensive metabolizers. L, R: left, right; n.s.: not significant. Significance levels are two-tailed.

Table 3. Voxel by voxel region of interest analysis, hippocampus and thalamus

Location	MNI Coord. x, y, z (mm.)	max *t*	*p* (vox. corr.)	*k*	*p* (cl. corr.)
Matched sample PM vs. EM					
Hippocampus L	−24 −30 −8	1.86	n.s.	28	n.s.
Hippocampus R	34 −26 −18	3.12*	n.s.	328	0.03
Thalamus L	−6 −16 18	3.16*	0.06	1697	0.002
Thalamus R	16 −12 −2	3.70*	0.02	s.c.	
Whole sample					
Hippocampus L	−16 −26 −12	2.64	n.s.	204	0.09
Hippocampus R	34 −26 −18	2.60	n.s.	166	0.13
Thalamus L	−4 −10 0	3.01*	0.06	1743	0.002
Thalamus R	6 −8 −2	3.39*	0.02	s.c.	

Abbreviations: EM, PM: extensive, poor metabolizer; MNI Coord.: Montreal Neurological Institute coordinates, in mm.; *p* (vox. corr.), significance level, voxel-level corrected with small volume hippocampi or thalami; *k*: cluster size, in 2 × 2 × 2 mm. voxels; *p* (cl. corr.), significance level, cluster-level correction for small volume hippocampi or thalami; L, R: left, right; s.c.: same cluster. The asterisk * denotes significance at voxel or cluster level, one-tailed.

Titles and legends to figures

Figure 1. Box plots of adjusted average perfusion levels in the regions of interest left and right hippocampus, left and right thalamus (from left to right) in the whole sample. The *CYP2D6* genotype codes are: EM for extensive metabolizer, IM for intermediate metabolizer and PM for poor metabolizers. Boxes are drawn at the lower and upper quartile values and, because of the very different number of observations in each group, are a better indication of the relatively constant variance across groups. The symbols X refer to observations beyond 1.5 times the interquartile range of the data (outliers). CBF: cerebral blood flow (in ml/100gr/min). L, R: left, right.

Figure 2. Box plots of adjusted average perfusion levels in the thalamus. On the *x* axis, CYP2D6 activity as according to ref. 37. Individuals with activity 0 in this plot are poor metabolizers. CBF: cerebral blood flow (in ml/100gr/min). The nonlinearity of this curve is significant as a quadratic term added to the linear CYP2D6 activity score ($t_{180} = 1.95$, $p = 0.05$, two-tailed).

Figure 3. Top half: map of the *t* values of the regression of perfusion values on the number of deficient activity *CYP2D6* alleles over the whole brain (whole sample), overlaid on a standard T1-weighted template brain. Left: sagittal slice illustrating association between *CYP2D6* genotype and perfusion levels in the hypothalamus and in the occipital/calcarine cortex (lingual gyrus); centre: frontal slice at $y = -31$ mm (Montreal Neurological Institute coordinates) across the hippocampus and the adjacent occipito/temporal cortex (lingual and fusiform gyrus); right: transversal slice across the thalamus at $z = 8$ mm. For illustration purposes, *t* values were thresholded at the significance level $p = 0.05$, uncorrected. L, R, A, P: left, right, anterior, and posterior. Bottom half: box plots of mean adjusted CBF perfusion in the hypothalamus ($t_{181} = 3.66$, $p < 0.001$) and occipital/calcarine region ($t_{181} = 3.52$, $p < 0.001$), divided by CYP2D6 activity scores as according to ref. 37. Individuals with activity 0 in this plot are poor metabolizers. CBF: cerebral blood flow (in ml/100gr/min).

Figure 4. Axial slices of the hippocampal formation (highlighted background), with overlaid *t* values, thresholded at the significance level $p = 0.05$, uncorrected (whole sample). The right side of the brain is on the right. The figure covers a range that in the anterior-posterior direction covers $y = 10$ to $y = -45$. A, P: anterior, posterior.

Figures

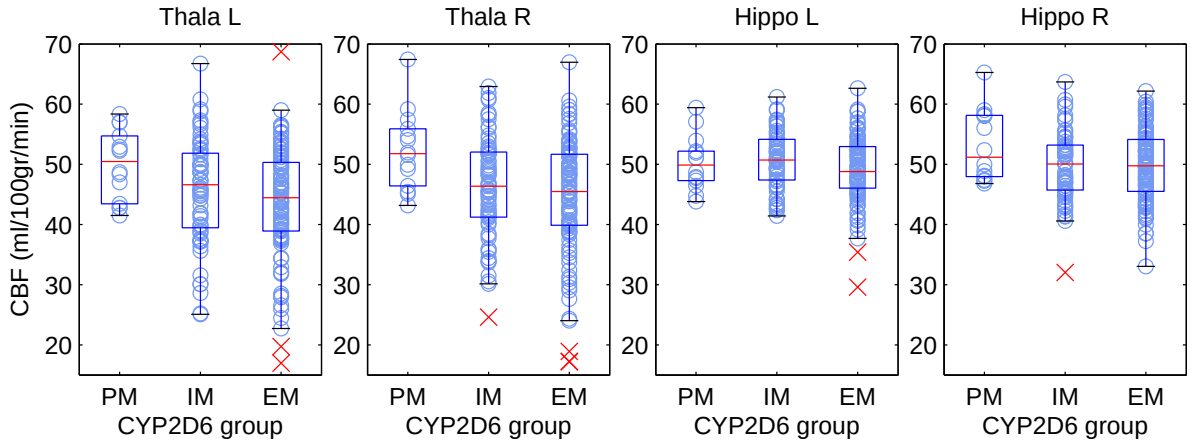

Figure 1

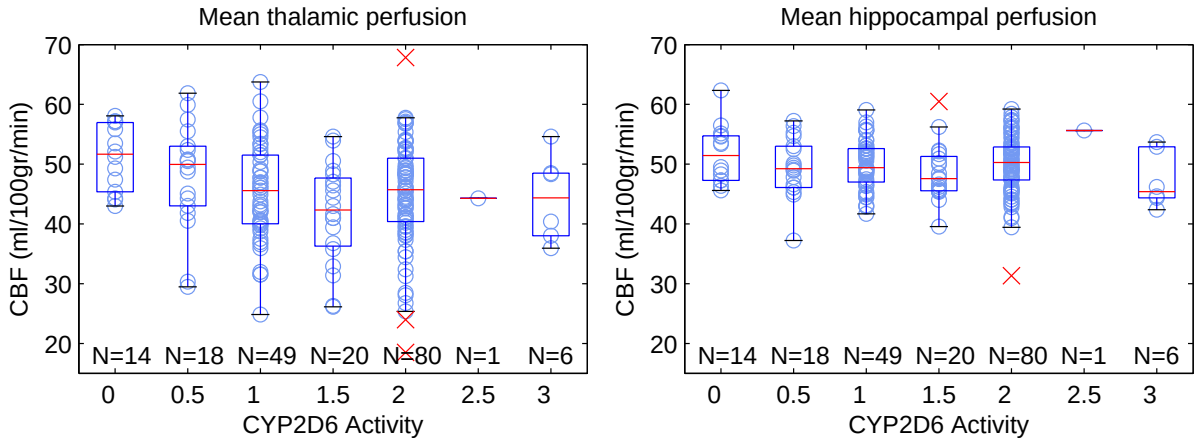
Mean thalamic perfusion
CBF (ml/100gr/min)
70
60
50
40
30
20
N=14 N=18 N=49 N=20 N=80 N=1 N=6
0 0.5 1 1.5 2 2.5 3
CYP2D6 Activity
Mean hippocampal perfusion
CBF (ml/100gr/min)
70
60
50
40
30
20
N=14 N=18 N=49 N=20 N=80 N=1 N=6
0 0.5 1 1.5 2 2.5 3
CYP2D6 Activity

Figure 2

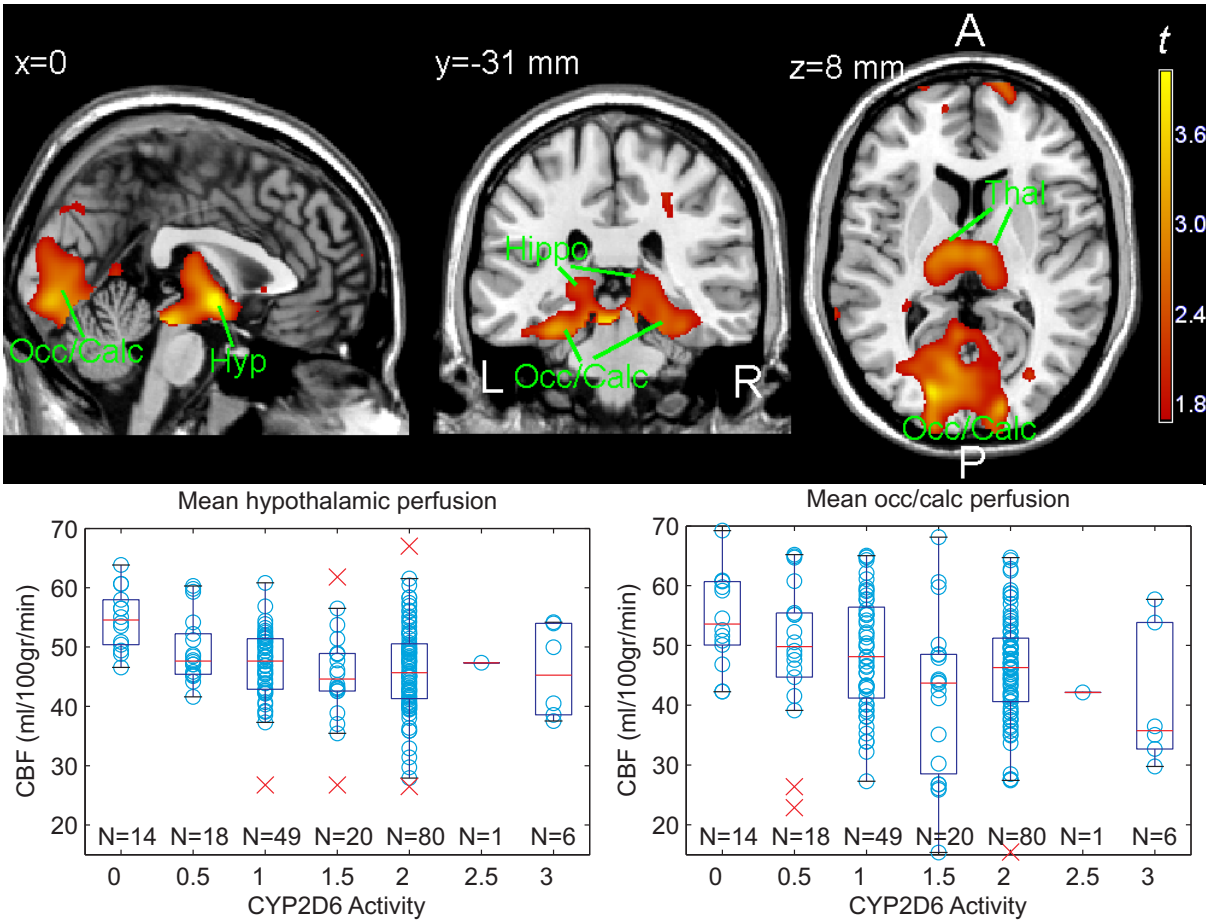
x=0
y=-31 mm
z=8 mm
A
P
L
R
t
3.6
3.0
2.4
1.8
Occ/Calc
Hyp
Hippo
Occ/Calc
Thal
Occ/Calc
Mean hypothalamic perfusion
CBF (ml/100gr/min)
70
60
50
40
30
20
N=14 N=18 N=49 N=20 N=80 N=1 N=6
0 0.5 1 1.5 2 2.5 3
CYP2D6 Activity
Mean occ/calc perfusion
CBF (ml/100gr/min)
70
60
50
40
30
20
N=14 N=18 N=49 N=20 N=80 N=1 N=6
0 0.5 1 1.5 2 2.5 3
CYP2D6 Activity

Figure 3

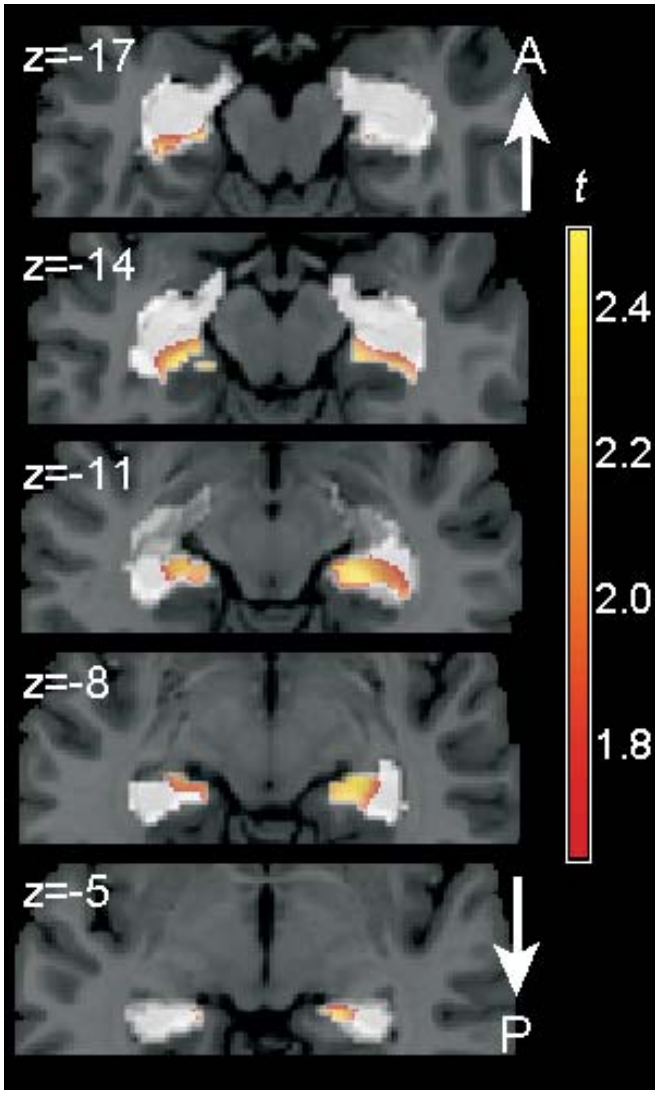

Figure 4